This is a repository copy of *Virus-induced changes in root volatiles attract soil nematode vectors to infected plants*.

White Rose Research Online URL for this paper:
https://eprints.whiterose.ac.uk/209335/

Version: Published Version

Virus-induced changes in root volatiles attract soil nematode vectors to infected plants

Pierre-Alain van Griethuysen[1]*, Kelly R. Redeker[1]* (iD), Stuart A. MacFarlane[2] (iD), Roy Neilson[3] (iD) and Sue E. Hartley[4] (iD)

[1]Department of Biology, University of York, Heslington, York, YO1 5DD, UK; [2]Cell and Molecular Sciences Department, The James Hutton Institute, Invergowrie, Dundee, DD2 5DA, UK; [3]Ecological Sciences Department, The James Hutton Institute, Invergowrie, Dundee, DD2 5DA, UK; [4]School of Biosciences, University of Sheffield, Western Bank, Sheffield, S10 2TN, UK

Summary

• Plant-derived volatiles mediate interactions among plants, pathogenic viruses, and viral vectors. These volatile-dependent mechanisms have not been previously demonstrated belowground, despite their likely significant role in soil ecology and agricultural pest impacts. We investigated how the plant virus, tobacco rattle virus (TRV), attracts soil nematode vectors to infected plants.

• We infected *Nicotiana benthamiana* with TRV and compared root growth relative to that of uninfected plants. We tested whether TRV-infected *N. benthamiana* was more attractive to nematodes 7 d post infection and identified a compound critical to attraction. We also infected *N. benthamiana* with mutated TRV strains to identify virus genes involved in vector nematode attraction.

• Virus titre and associated impacts on root morphology were greatest 7 d post infection. Tobacco rattle virus infection enhanced 2-ethyl-1-hexanol production. Nematode chemotaxis and 2-ethyl-1-hexanol production correlated strongly with viral load. Uninfected plants were more attractive to nematodes after the addition of 2-ethyl-1-hexanol than were untreated plants. Mutation of TRV RNA2-encoded genes reduced the production of 2-ethyl-1-hexanol and nematode attraction.

• For the first time, this demonstrates that virus-driven alterations in root volatile emissions lead to increased chemotaxis of the virus's nematode vector, a finding with implications for sustainable management of both nematodes and viral pathogens in agricultural systems.

Introduction

Plants are under constant attack from a range of organisms, both above- and belowground (War *et al.*, 2012). These ecological interactions are significant for ecosystem structure with both predator–prey (top-down) and producer–consumer (bottom-up) interactions often chemically mediated (Raguso *et al.*, 2015). This mediation takes the form of small molecule metabolism, which controls information transfer between organisms, both aboveground and in soils (Bouwmeester *et al.*, 2019). Identification and quantification of volatile chemical cues that drive multitrophic interactions associated with plants is necessary for better understanding of ecosystem dynamics, and for sustainable pest control strategies (Pickett & Khan, 2016).

Plant viruses are among the most devastating of natural plant antagonists, particularly in agricultural systems in which they are one of the most significant threats to crop production (Jones & Naidu, 2019). An important step in reducing viral impacts on food security is to obtain a better understanding of

chemical signals that underpin viral transmission; viruses rely on attracting their vectors to infected plants, and this attraction is commonly through plant-derived volatile signals (Mauck *et al.*, 2010; McMenemy *et al.*, 2012) although in aboveground interactions other, visual signals can also be important. In aboveground plant virus–vector interactions, viruses are known to maximise their fitness by manipulating both host–plant signals and vector behaviour to make infected plants more attractive to vector organisms than uninfected plants (Mauck & Chesnais, 2020). This enhanced attraction is caused by changes in the total amount and/or relative concentrations of the blend of volatiles emitted by infected, aboveground plant tissues (Eigenbrode *et al.*, 2018). Crucial cues for host selection by vectors can result from viral modifications of infected plant emissions (Fereres *et al.*, 2016).

While plant-mediated processes underpinning increased attraction of insect vectors to infected plants aboveground have been well-characterised (Shapiro *et al.*, 2012), little is known about chemical cues mediated by viruses that are transmitted by non-insect, belowground vectors. This is a significant knowledge gap, particularly in the case of soil nematodes, which play a

---

*These authors contributed equally to this work.

critical role in soil function and ecosystem processes (Bardgett & van der Putten, 2014). Nematodes are diverse and abundant; one of the largest phyla in the animal kingdom and occupying diverse environments across the globe with plant-pathogenic and bacterial-feeding nematode species functionally dominant in soils (van den Hoogen *et al.*, 2019). Nematodes are critical in driving soil functional behaviour, impacting soil food webs, soil carbon cycling, plant nutrient uptake, plant community dynamics and aboveground biodiversity (Bezemer *et al.*, 2005; De Wang *et al.*, 2019), but despite these essential roles, studies on soil nematode interactions and behaviour remain under-represented (Lazarova *et al.*, 2021).

Plant-pathogenic nematodes are devastating agricultural pests (Chitwood, 2003). Trichodorid nematodes (Fig. 1) are ectoparasitic (all life stages exterior to the plant host), pathogenic root-feeding nematodes of which some species act as the vector for the tobraviruses, TRV, pea early-browning virus (PEBV) and pepper ringspot virus (PepRSV; Taylor & Brown, 1997; MacFarlane, 1999). Tobacco rattle virus, a commercially important pathogen of cultivated potato (*Solanum tuberosum*), reduces crop quality and causes it to be unmarketable (Otulak *et al.*, 2012; Sahi *et al.*, 2016; Fig. 1). Trichodorid feeding on infected plant roots, and then on uninfected host roots, is the known mechanism by which TRV is transmitted within crops. However, to date, details of the physical and chemical interactions between nematodes and virus-infected plants remain opaque.

Over 400 plant species are known to be susceptible to TRV infection (MacFarlane, 2008). In common with other plant virus infections (Nibau *et al.*, 2008), nematode-mediated plant infection by TRV leads to fitness consequences for the plant with altered root morphology and root structure architecture (Taylor & Brown, 1997). Direct damage through trichodorid feeding typically results in shortening and thickening of plant roots (Christie & Perry, 1951) with a concomitant overall reduction in root development (Boutsika *et al.*, 2004). For several plant-parasitic nematode taxa, this is coupled with modified plant nutrient and water uptake, leading to stunted growth, leaf chlorosis, and wilted foliage (Decraemer, 1995; Jones *et al.*, 2010) and in potato, reduced yields, and tuber necrosis (Beuch *et al.*, 2014). Trichodorid transmission of TRV is achieved through physical binding of virus particles to the stylet, a hollow feeding tube that the nematode uses to penetrate root cells; it is a complex biological process underpinned by specific virus serotype-nematode

species combinations (Ploeg *et al.*, 1992). Non-specific transmission of TRV by non-trichodorid nematodes does not occur.

Nematodes, including trichodorids, orientate themselves towards host plants using chemical cues, aggregating at the elongation zone of growing roots (Taylor & Brown, 1997), possibly in response to root exudates. Root metabolites are known to attract nematodes towards roots (Sikder & Vestergård, 2020), but those nematode species so far shown to be affected by these signals are exclusively endoparasites that have a period of their life cycle located within the plant host. For example, a recent study demonstrated that benzoxazinoids, soluble secondary metabolites found in the root exudates of many cereal crops, differentially affected the abundance of endoparasitic root-associated nematode taxa in maize (Sikder *et al.*, 2021). Nematodes are also attracted to a range of volatile compounds which, while only forming *c.* 1% of all root-released exudates (Venturi & Keel, 2016), easily diffuse through gas- and water-filled pores and therefore have a wider range in soils than water-soluble, non-gaseous exudates (Rasmann *et al.*, 2012; Schulz-Bohm *et al.*, 2018). Long-range volatile attractants of trichodorids remain unidentified, and the role of these chemical cues in attracting key vectors to virus-infected plants has not been tested.

The TRV genome is composed of two single-stranded, positive-sense RNAs, encapsidated separately in rod-shaped particles of different lengths (MacFarlane *et al.*, 1999; Fig. 2). Early work on TRV identified two different types of infection: non-multiplying (NM) and multiplying (M; Harrison & Robinson, 1978). Non-multiplying infections occur when only RNA1 is present, do not produce virus particles and are non-transmissible by trichodorids. Nevertheless, RNA-1 encodes all the virus proteins necessary for replication and movement in the plant. M-type infections carry both RNA1 and RNA2, and as RNA2 encodes the coat protein (CP) such infections produce virus particles. In some TRV isolates, RNA2 encodes the non-structural proteins, 2b and 2c. 2b has been demonstrated to be involved in transmission of TRV by trichodorid nematodes (Hernández *et al.*, 1997; Vassilakos *et al.*, 2001). The 2c gene was not required for transmission of TRV but was involved in the transmission of another tobravirus, PEBV (MacFarlane *et al.*, 1996).

This knowledge, and the recent development of systems to manipulate and modify the TRV genome in pre-determined ways, makes it possible to use the TRV-tobacco-trichodorid

Fig. 1 Effect of tobacco rattle virus (TRV) on potato tubers, showing necrotic rings common of spraing disease/corky ringspot and a trichodorid nematode, vector of TRV (images by R. Neilson).
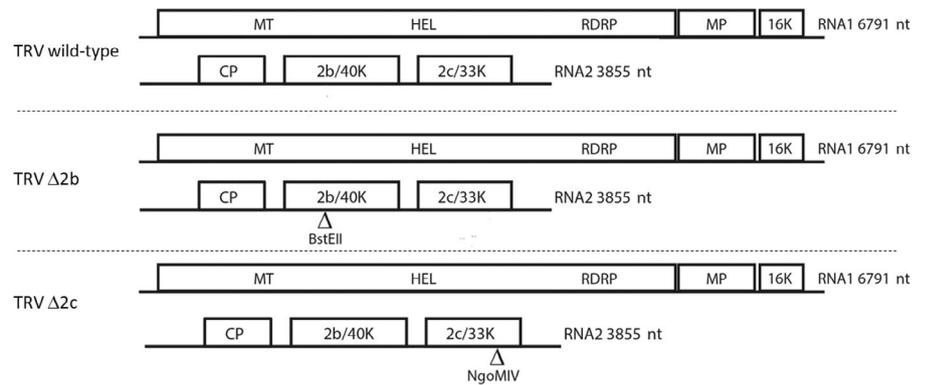
Fig. 2 Genome organisation of tobacco rattle virus (TRV) isolate PpK20 showing the locations of the 2b and 2c mutations in RNA2. Protein functions (where known) are noted; MT, methyltransferase; HEL, RNA helicase; RDRP, RNA-dependent RNA polymerase; MP, movement protein; CP, coat protein. ΔBstEII and ΔNgoMIV show the locations of the 2b and 2c gene frameshift mutations introduced separately into RNA2 during this work.

nematode pathosystem as a model system with which to investigate the belowground chemical and biological interactions between the virus and its nematode vector.

In this study, we hypothesized that:
(**1**) Viral infection impacts root growth, morphology and the release of volatiles from infected roots, and that these changes would correlate with the level (titre) of virus infection;
(**2**) Trichodorids will be more attracted to virus-infected plants, and the greater attraction will be driven by infection-induced changes in the quantity and composition of the plant volatile signature; and
(**3**) Loss of function in TRV RNA2 genes through mutation would impact the observed changes in plant roots and root volatiles in response to virus infection and hence alter the response of trichodorids to infected plants.

Materials and Methods

TRV clones and mutant design

Tobacco rattle virus of isolate PpK20 was used in this study and was derived from a set of wild-type (wt) and mutated cDNA clones inserted in binary plasmids that were transformed into *Agrobacterium tumefaciens* (Smith & Townsend) Conn strain GV3101. pTRV1, an infectious clone of TRV PpK20 RNA1, was described by Liu *et al.* (2002). The wt clone of TRV PpK20 RNA2 (p1466) was constructed by replacing the RNA1 sequence from pTRV1 with the complete TRV RNA2 sequence from the infectious transcript clone of Mueller *et al.* (1997) (pT72K20). Two frameshift mutations were created separately in the 2b gene and in the 2c gene carried on pT72K20. The entire TRV RNA2 from these mutants was amplified by PCR and cloned using the NEBuilder HiFi Assembly kit (New England Biolabs, Ipswich, MA, USA) into the small, low copy number binary vector pDIVA (Laufer *et al.*, 2018). The 2b gene frameshift was created by the digestion of pT7K20 with BstEII, followed by blunting using Klenow polymerase and relegation, resulting in the insertion of an additional five nucleotides (nt). The 2c gene frameshift was created by digestion of pT7K20 with NgoMIV, followed by blunting using Klenow polymerase and relegation, resulting in the insertion of an additional 4 nt. Both mutations interrupt translation of the frameshifted gene and are expected to abolish

gene function. Clone p1795 carries TRV RNA2 with the 2b gene mutation, which is denoted as Δ2b. Clone p1796 carries TRV RNA2 with the 2c gene mutation, which is denoted as Δ2c.

Plant growth and infection

Nicotiana benthamiana Domin seeds were sterilised by exposure to 100% ethanol (2 min), followed by centrifugation (5 *g*-force for 2 min) to remove ethanol and addition of 50% commercial bleach solution. The bleach and seed solution were left for 15 min then centrifuged (5 *g*-force for 2 min), the bleach removed, and the seeds rinsed five times with dH$_2$O. Seeds were germinated on moist filter paper at 20°C, then transferred to trays of 90 : 10 mix of autoclaved sand : John Innes #2 compost. Seedlings were watered with ½ strength modified Hoagland's nutrient solution until two true leaves had expanded. Thereafter, the plants were potted in different media, depending on the experiment.

Plants for root architecture and volatile collection assays were planted in 1-l pots of washed and autoclaved sand while plants for trichodorid preference tests were directly planted into 50-ml olfactometer pots containing washed and autoclaved sand that was kept at 20% moisture by volume until the start of the trials. Pots were not handled during the trials to avoid disturbance.

To infect the *N. benthamiana* plants with TRV, agrobacterium cultures carrying the TRV RNA1 and TRV RNA2 (wt and mutant) clones were grown overnight at 28°C, the cells were collected by centrifugation and resuspended at an OD$_{600}$ of 0.1 in infiltration buffer containing acetosyringone (Ratcliff *et al.*, 2001). Equal volumes of TRV RNA1 and TRV RNA2 (wt or mutant) were combined and infiltrated using a needle-less syringe into the apoplast below the lower epidermis of three randomly selected leaves of each plant at the six true-leaf growth stage. Control plants were infiltrated with a suspension of agrobacterium not transformed with any of the virus binary plasmids.

Plants were thereby infected with one of three different treatments (Fig. 2) as soon as six true leaves were present (between 10 and 14 d postgermination):
(**1**) 'TRV Wild-type' plants infected with TRV RNA1 and wt TRV RNA2.
(**2**) 'TRV Δ2b' plants infected with TRV RNA1 and mutant TRV RNA2 incorporating a silenced 2b gene.

(**3**) 'TRV Δ2c' plants infected with TRV RNA1 and mutant TRV RNA2 incorporating a silenced 2c gene.

Control plants ('uninfected') were inoculated with untransformed *Agrobacterium*. Infection solutions were prepared by making overnight stocks of each culture from frozen glycerol stocks and preparing infiltration cultures of mixed RNA-1/RNA-2 or untransformed *Agrobacterium*. Once mixed, 0.5 ml of the combined infiltration medium were inoculated onto the apoplast of each leaf using a needle-less syringe (Senthil-Kumar & Mysore, 2014). Three leaves, selected at random, were inoculated per plant.

Successful plant infection was confirmed with end-point RT-PCR assays on leaf and root tissue from infiltrated plants using RNA1-(16K gene)-specific and RNA2 (PPK20 CP gene)-specific primers developed by Boutsika *et al.* (2004). Quantification (qRT-PCR) of viral infection used RNA1-specific primers 2353 (TACCAAGGGAATGTGTTCTA) and 2354 (CTCGGAAC TCCAGCTATC), which amplify a 91-bp fragment of the viral replicase gene and was normalised against two *N. benthamiana* reference genes (APR and EF1α; Liu *et al.*, 2012).

Growth and root morphology

One hundred *N. benthamiana* plants were potted into 1-l sand-filled pots to establish root morphological effects arising from TRV infection. *Nicotiana clevelandii* or *N. benthamiana* are often used as a virus source and transmission bait plants, as these species are highly susceptible to virus infection. *Nicotiana benthamiana* was used in this instance because it is very susceptible to TRV, becoming systemically infected very quickly (MacFarlane & Neilson, 2009). Plants were fed with 250 ml ½ strength Hoaglands twice weekly and watered with dH$_2$O daily. To quantify the full TRV infection time course, plants were sampled at 4, 7, 14, 21, and 28 d post infection (dpi). Five plants per treatment (Uninfected, TRV wt, TRV Δ2b, and TRV Δ2c) were harvested at each time point by carefully rinsing away the supporting sand. Plants were weighed, and root architecture parameters (root and shoot fresh weight, total root length, total root surface area, total root volume, number of tips, and degree of root branching, i.e. tip number divided by total root length) were measured by scanning carefully spread root systems within a thin layer of water on a transparent tray. Once roots were scanned, they were dried at 60°C until constant weight (change < 0.01 mg dy^{-1}). Scanned images were analysed using the WINRHIZO software (Regent Instruments, Quebec City, QC, Canada) using a skeletonisation method (Himmelbauer, 2004).

Root VOC sampling

Twenty *N. benthamiana* plants were grown in 1-l sand-filled pots and watered twice weekly with a ½ strength Hoagland's solution regimen to quantify root volatile impacts arising from TRV infection. Plants were either uninfected or infected with TRV wt, TRV Δ2b, or TRV Δ2c. Root volatile samples were collected, during the period of maximum infection, at 7 dpi.

Plants (7 dpi) were placed in a sampling chamber that isolated the plant roots in a sealed space (Supporting Information Fig. S1) from the rest of the plant. A ¼″ stainless steel line from the isolated airspace (I, Fig. S1) was connected to an Ascarite trap (III, Fig. S1) which connected to a 500-ml sampling canister (IV, Fig. S1). Ascarite traps were used a maximum of four times before replacement. A 1/8″ diameter hole at the back of the chamber allowed ambient air to replace the air taken at each sample (V, Fig. S1), avoiding depressurisation of the plant roots in the chamber but diluting the measured volatile outputs slightly. Between samples, the valve (II, Fig. S1) connecting to the Ascarite trap was closed to prevent ambient air flow into the chamber. Fitted silicon discs sealed with high vacuum silicon grease (Dow Corning GMBH, Wiesbaden, Germany) separated aboveground and belowground plant components.

Our reported plant volatile flux (grams of compound per minute) is calculated from the change in headspace volatile concentration (as described in Eqn 1) divided by dry root weight.

$$\text{Flux} \left(\text{g min}^{-1} \right) = \frac{\text{CH}_{T60} - \text{CH}_{T0}}{t_{60} - t_0} \qquad \text{Eqn 1}$$

Here, CH$_T$ is the mass of the compound of interest in the sampling chamber at time points 0 and 60 min, while t represents the time of sampling in minutes. To obtain these values, volatile samples were taken within 1 min (time = 0), providing a baseline sample of background air, and at 60 min (time = 60). This approach automatically identifies and removes background contaminants from consideration, since they will not change in concentration over the course of the sampling procedure unless they are metabolised by the roots within the sampling apparatus.

Volatiles were collected in pre-evacuated (< 0.02 mbar) stainless steel electropolished canisters (LabCommerce Inc., San Jose, CA, USA), stored at 20°C and analysed within 2-wk after sampling (Low *et al.*, 2003). Samples were directly transferred from the canisters onto a liquid nitrogen condensation trap via pressure differential (trap pressure < 0.02 mbar; Redeker *et al.*, 2018), then re-volatilised in a 100°C water bath and transferred to an Agilent 6890 gas chromatograph-mass spectrometer (GC : MS) using a DB-5 column (30 m × 0.32ID × 5 μm; Agilent, Santa Clara, CA, USA). Samples were run using a scanning method (which quantified fragment masses between 50 and 200 atomic mass units) with an initial oven temperature of 30°C, held for 5 min, first ramp of 4°C min^{-1} to 250°C (no hold) and a second ramp and bake-out of 40°C min^{-1} to 325°C with a 5-min final hold (total runtime of 66 min). The mass range was chosen to avoid carbon dioxide and water contamination (baseline elevation leading to sensitivity reduction) while maximising sensitivity for lower mass volatiles, which more rapidly diffuse in soils. Compounds with masses > 200 amu were detectable/identifiable due to compound fragmentation at the source but were not produced in substantial quantities or, in the specific case of β-caryophyllene, not produced by the plants at all (Fig. S2). β-caryophyllene has been identified as an important signalling compound in entomopathogenic nematode ecology (Turlings *et al.*, 2012) and was therefore injected directly using serial

dilution of known standards to confirm retention time and system sensitivity.

Compounds for which control plants and virus-infected plants had statistically similar responses (ANOVA, $P > 0.05$) were deemed either to be common biogenic metabolites, chamber-generated volatiles, or stress response volatiles common to infected and uninfected plants (Fig. S2). These compounds were neither identified nor quantified. The remaining compound of interest, that is the compound expressed in virus infected but not control plants, was tentatively identified using standard NIST library spectra comparison, and identity confirmed with injections of purchased standards (Sigma-Aldrich; Fig. S2). Quantification of compound concentration (to parts-per-trillion-by-volume, or pptv) was performed using serial dilution standards from purchased, neat standards (as described in Issitt *et al.*, 2022), with a detection limit of *c.* 8 pptv. Compound concentration was transformed to chamber headspace amount (grams of compound; Eqn 1) by multiplying pptv concentration by the molar amount of air in the headspace and dividing by one trillion.

Trichodorid preference

Trichodorid preference testing was carried out in purpose-built olfactometers, constructed of cut 50-ml plastic tubes and PTFE tubing (Fig. 3). Two PTFE 'arms', which consisted of two sections: a 50 mm section connected to the central pot and leading towards the outer pots was blocked at its outer end by a 2 μm mesh (TWP Inc., Berkeley, CA, USA) and a 30 mm portion of PTFE completed the connection to the outer pots. Each olfactometer had two outer pots with a plant in each, allowing two different treatments to be compared. Treatments (left or right pot) were randomly allocated for each replicate pair in each treatment. Olfactometers and the PTFE arms were filled with dH₂O washed and autoclaved sand that was kept at 20% moisture by volume until the start of the assay. Nematode communities including trichodorids were extracted from a 200 g subsample (Wiesel *et al.*, 2015) from agricultural soil using a modified Baermann funnel extraction method (Brown & Boag, 1988). After *c.* 48 h, extracted nematodes were collected in 20 ml of water and left to settle for *c.* 2 h and excess water decanted. Trichodorids were identified using morphological features under a low-powered

Fig. 3 Design of olfactometers. Trichodorids moving towards uninfected or tobacco rattle virus (TRV)-infected plants; nematodes were collected from the arms of the olfactometer leading to plants from those treatments and are prevented from escaping from the arms by a 2 μm mesh.

microscope and individually hand-picked from the extracted nematode communities into distilled water in 2-ml Eppendorf tubes and stored at 4°C until required. Trichodorids were added to the central pot when the plants in the flanking pots had reached 7-d postinfiltration with the agrobacterium (+/− TRV) suspension(s). The clear plastic pots were wrapped in aluminium foil to exclude light, with the foliage of the plants remaining uncovered, and the experiment was kept at 23–24°C throughout the experiment. Four replicate sets of 50 trichodorids were used, and each experiment was carried out twice, apart from the TRV wt vs uninfected preference test, which was carried out three times.

To test trichodorid response to 2-ethyl-1-hexanol, an amended olfactometer design was used, with a glass capillary present in each planted, outer pot. The capillary allowed liquid 2-ethyl-1-hexanol to be added to the root system of one of the plants where it would equilibrate between vapour and liquid phases, diffusing via the gaseous phase of the sand matrix into the tubes connecting to the central pot where the trichodorids were initially placed. Release of 2-ethyl-hexanol from *N. benthamiana* plants at 7-d postvirus infection was calculated, based on chamber headspace, root volatile emissions and average root mass at 7 d, to be 31–67 μg per plant over 48 h. Doses of 2-ethyl-1-hexanol were calculated so that over the run, 200× this estimate was added to each pot over the course of the 2-d experiment, allowing for accelerated losses from both capillary and sandy soil surface and the potential for reduced sensitivity due to chiral-specific nematode response. We thereby increased the likelihood of nematode response and analytical detection. A total of 160 μl of 2-ethyl-1-hexanol standard (Sigma-Aldrich, 833 kg m⁻³) was added. To the 2-ethyl-1-hexanol treated plant, 16 μl of standard were added via the capillary at 0, 4, 24 and 28 h; with 48 μl added at 8 and 32 h. Trichodorid olfactometer response experiments tested whether wt-infected plants were more attractive to nematodes than uninfected control plants, and relative responses of nematodes to uninfected plants and those infected with the least-productive mutant (Δ2b, both with and without 2-ethyl-1-hexanol addition) to wt infection.

At the conclusion of each experiment, the tubing 'arms' leading away from the central pot towards the flanking pots with plants were collected. The mesh placed at the end of these tubes adjacent to the outer pots prevented the nematodes from moving into the plant pots and enabled them to be collected as described above and counted.

Statistical analysis

Data from two or three repeats of the trichodorid olfactometer experiments were pooled and analysed with a generalised linear model (GLM) with Poisson regression. The assumptions of the model were checked, and a deviance goodness-of-fit test was conducted to ensure the appropriate GLM family was used, which was only accepted if the result was > 0.8 (Wood *et al.*, 2020). Overdispersion was also tested using the Applied Econometrics for R package (Kleiber & Zeileis, 2008). Trichodorid count was set as the dependent variable while sample number and
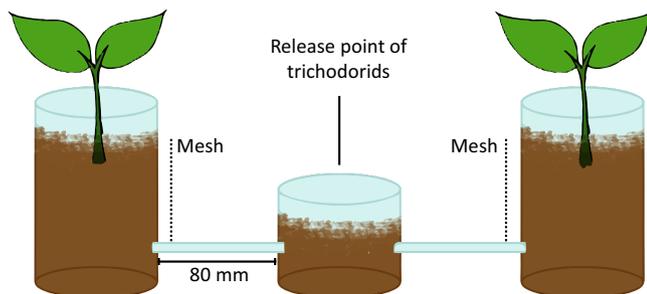
experimental repeat (to account for the pooling of data) were set as independent variables. Models including only sample number as the independent variable had better Akaike Information Criteria, so this was the only variable used in the final model. An analysis of deviance was performed on the model with Tukey HSD *post hoc* tests with *P* value adjustment to investigate significance. Comparisons between 2-ethyl-1-hexanol emissions and virus RNA level was carried out with linear regression. All other data were analysed using analysis of variance (ANOVA) and model assumptions checked with Shapiro–Wilk and Levene's tests for normality and homogeneity of variance, respectively. All root architecture parameters and qPCR data were transformed using cube root transformation to fit the analysis of variance assumptions. Root architecture data were analysed per time point, as well as across the entire data set. Tukey's HSD *post hoc* tests were used when two or more levels of an interaction were significant. Statistical analysis was carried out in R (R Core Team, 2020). The packages *car*, *arm*, and *emmeans* were used for the linear mixed effects model, whereas *car*, *rcompanion* and *MASS* were used for data transformation and visualisation.

Results

Impacts of TRV Infection on *N. benthamiana* root morphology

Tobacco rattle virus infection, whether by the wt virus or the 2b and 2c mutants, significantly altered the measured root parameters, but only for a limited period: The significant changes observed at 7 and 14 dpi were no longer observed by 21 dpi (Table S1). Plants infected by wt TRV showed a reduction in root dry weight and root length, volume, and surface area at both 7 and 14 dpi (Table S1; Fig. 4a).

Plants infected with the TRV mutants showed slightly different responses in terms of impacts on their root growth and morphology compared with infection by the wt virus (Table S1). For example, at 7 and 14 dpi, plants infected with TRV Δ2c had reduced root dry weights compared with uninfected plants, but greater root dry weight than wt virus-infected plants, whereas plants infected with TRV Δ2b were also reduced in root dry weight relative to uninfected ones but did not differ from wt TRV-infected plants (Table S1). Tobacco rattle virus Δ2b infection reduced root length compared with uninfected and TRV Δ2c infected plants in a manner similar to wt virus infection. In terms of root surface area, both mutant virus infections showed reductions compared with uninfected plants at 7 dpi, but only TRV Δ2c infected plants were different to plants infected with the wt virus (Fig. 4a). By 14 dpi, root surface area in TRV Δ2c infected plants was no longer reduced compared with uninfected plants, nor did it differ significantly from that of wild-type infected plants. Overall, TRV infection temporarily reduces the relative size of whole plant root systems.

The amount (titre) of virus accumulated in the infected plants changed over the course of the infection and followed the same pattern as was found for the root morphology changes, with maximum infection at 7 dpi, and significantly reduced, but still
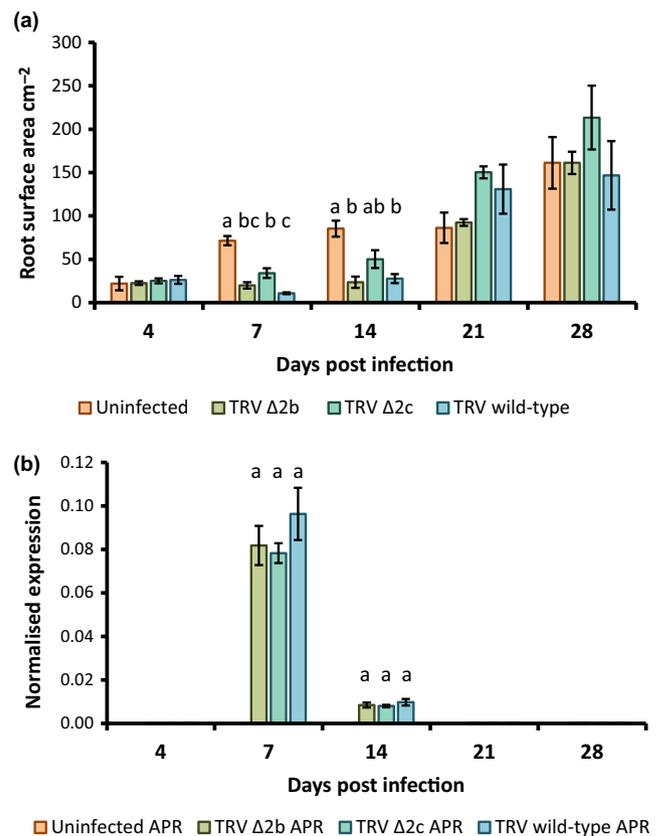

Fig. 4 Effect of infection with wild-type tobacco rattle virus (TRV) and frameshift mutants on root surface area across the 28-d infection timeline. (a) Differences of root surface area in *Nicotiana benthamiana* plants infected with different TRV treatments. Significant differences between treatments were only seen at 7 and 14 d post infection (statistically similar/ differing groupings are annotated with differing lowercase letters above columns, Day 7: $F(3,16) = 25.27$, $P < 0.001$; Day 14: $F(3,16) = 8.38$, $P < 0.01$). Seven days post infection: uninfected plants had greater surface area than TRV Δ2b ($P < 0.001$), TRV Δ2c ($P < 0.01$) and wild-type infected plants ($P < 0.001$) while TRV-Δ2c infected plants had greater surface area than wild-type infected plants ($P < 0.01$). Fourteen days post infection: only significant differences were between uninfected and TRV-Δ2b ($P < 0.01$) and wild-type ($P < 0.01$) infected plants. (b) Normalised expression of TRV coat protein gene in *N. benthamiana* roots across the 28-d infection timeline. Changes in expression of a TRV gene normalised to a *N. benthamiana* housekeeping genes (APR) over course of infection. There was a significant increase in viral load 4–7 d post infection, with a significant, consecutive decrease in viral load at 14 and 21 d post infection. No significant differences were observed between TRV-infected treatments on any single date post infection. Means and standard errors are shown, $n = 5$ for all bars.

present infection at 14 dpi. By 21 and 28 dpi, there was no detectable TRV infection present in the plants (Fig. 4b). However, no significant differences in virus titre were observed between the wt and mutant viruses at 7 and 14 dpi.

Modifications of root volatile emissions by TRV infection

Root volatiles detected by the GC–MS analysis ranged from one to 20 carbons in size. 2-ethyl-1-hexanol (H_3C⌇⌇OH, CH_3) was the only compound in this analysis that showed consistent, large

differences in emissions between infected and uninfected plants. The roots of wt-infected plants released significantly (c. 14 times) more of this compound than uninfected plants (Fig. 5a; wt: 117.7 ± 19.0 ng min^{-1} g^{-1} root dry weight; uninfected: 8.4 ± 4.9 ng min^{-1} g^{-1} root dry weight). In wt virus-infected plants, normalised viral load explained nearly all the observed variance in 2-ethyl-1-hexanol emissions (Fig. 5b).
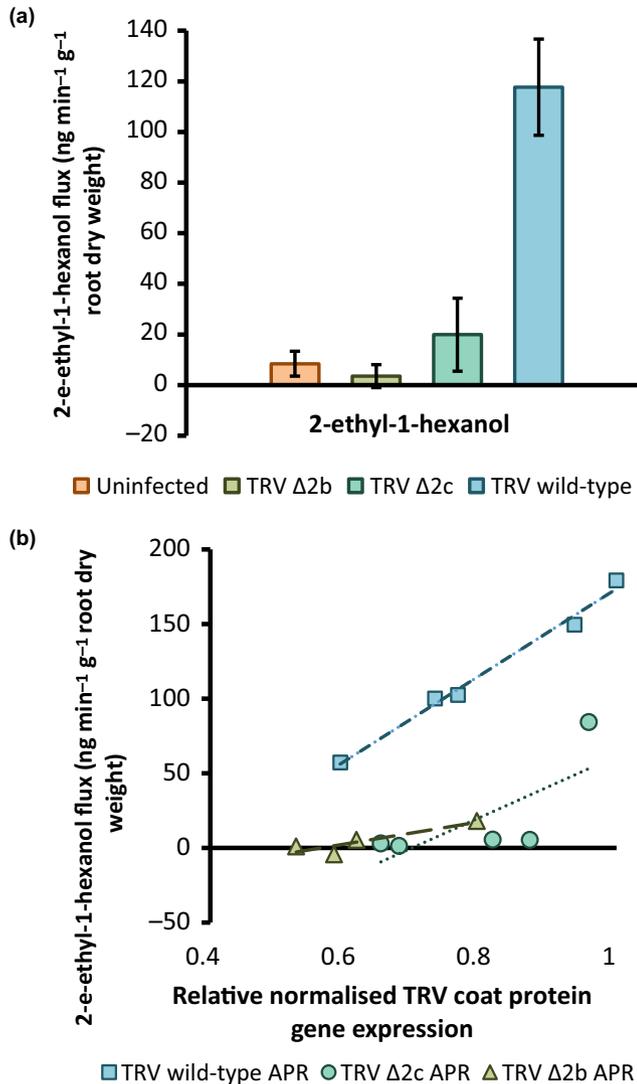

(a)

(b)

Fig. 5 2-Ethyl-1-hexanol emissions from the roots of uninfected plants and plants infected with tobacco rattle virus (TRV) and their relationship with viral load. (a) Mean 2-ethyl-1-hexanol VOC fluxes from the roots of uninfected plants and those infected with wild-type TRV and the TRV Δ2b and TRV Δ2c mutant lines. Error bars are standard error ($n = 5$). Emissions between TRV wild-type infected plants and other treatments differed ($P < 0.01$ compared to control and TRV-Δ2b, and $P < 0.05$ compared to TRV-Δ2c). (b) Relationship of 2-ethyl-1-hexanol flux with viral load in the root tissue. Comparison of root volatile emissions from plants infected with wild-type TRV and TRV Δ2b and TRV Δ2c mutant lines, with relative viral load normalised to a *Nicotiana benthamiana* housekeeping gene, APR. A significant relationship exists for wild-type infected plants ($r^2 = 0.99$; $P < 0.001$) and TRV Δ2b infected plants ($r^2 = 0.92$; $P < 0.01$), but not for the TRV Δ2c infected plants ($P = 0.16$).

The rate of emission of 2-ethyl-1-hexanol from plants roots infected with the Δ2b and Δ2c mutant viruses was similar to those in uninfected plants and was reduced relative to those infected with wt TRV (Fig. 5a). While emissions were reduced in Δ2b-infected plants, they were still correlated with viral load (Fig. 5b). Viral load, in terms of relative normalised expression of the TRV coat protein gene, was similar across the three infection treatments (Fig. 5b).

Trichodorid preference for TRV-infected plants

The treatments in the olfactometer preference experiment (Fig. 3) significantly affected trichodorid accumulation in the collection tubes (GLM-p $\chi^2_{(2,30)} = 88.8$, $P < 0.001$), with trichodorids preferentially moving towards the wt TRV-infected plant (Fig. 6a) when given the choice between that and an uninfected plant. Double the number of trichodorids moved towards the infected (8.4 ± 0.7 nematodes cm^{-3}) than the uninfected (4.2 ± 0.5 nematodes cm^{-3}) plants. Movement of trichodorids was positively correlated with increasing levels of viral load (Fig. 6b).

Trichodorid attraction to 2-ethyl-1-hexanol

To test the role of 2-ethyl-1-hexanol in trichodorid attraction, an amended olfactometer design was used (Fig. 7a). Attractiveness of uninfected plants, with and without the addition of 2-ethyl-1-hexanol, differed (Fig. 7b; GLIM-p $\chi^2_{(2,21)} = 12.4$, $P < 0.05$): More trichodorids moved towards the uninfected plants with added 2-ethyl-1-hexanol than towards those without, suggesting that the infection-induced increase in 2-ethyl-1-hexanol released from roots is an important chemical cue attracting trichodorids to TRV-infected plants.

In olfactometer assays to test the impact of mutation of the RNA2 2b gene on the attractiveness of infected plants to trichodorids, there was a significant difference in direction of trichodorid movement (GLM-p $\chi^2_{(2,21)} = 55.89$, $P < 0.001$, *post hoc P* < 0.05), with preference for wt TRV-infected plants rather than for plants infected with the Δ2b mutant virus (Fig. 7c). There was no significant difference in attractiveness when plants infected with TRV Δ2b were compared with uninfected plants (8.1 ± 1.2 vs 6.9 ± 1.0 nematodes cm^{-3} for Δ2b vs uninfected plants, respectively).

We also tested in olfactometer assays whether the addition of 2-ethyl-1-hexanol restored attractiveness to the TRVΔ2b mutant infected plants relative to wt TRV infection. A significant difference (GLIM-p $\chi^2_{(2,21)} = 55.9$, $P < 0.001$) in preference remained, with trichodorids moving in greater numbers towards wt-infected plants (Fig. 7c).

Discussion

This study has demonstrated that TRV-driven alterations in root volatile emissions lead to increased chemotaxis of the virus's trichodorid nematode vector and has identified the dominant chemical component of the signal manipulated by TRV to attract
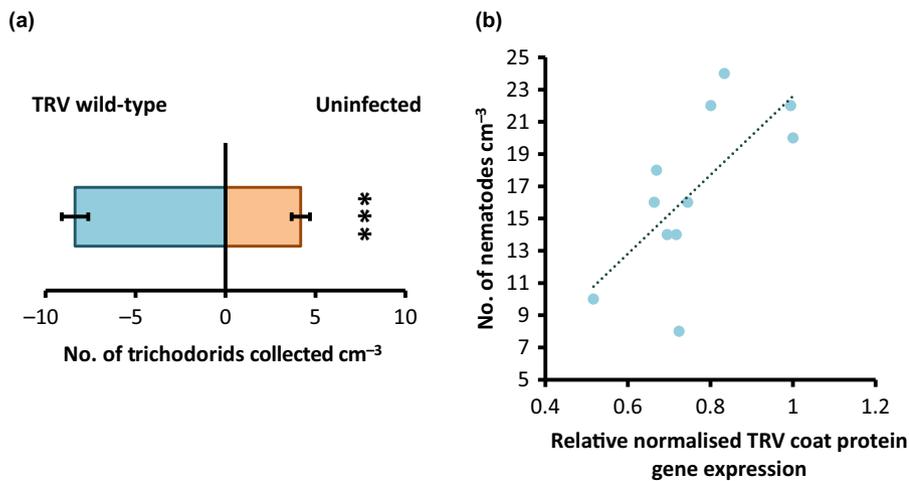
(a)

(b)

Fig. 6 Response of trichodorid nematodes when presented with uninfected and wild-type tobacco rattle virus (TRV)-infected plants. (a) Preference between uninfected and TRV wild-type infected plants is significant (GLM-p $\chi^2_{(2,30)} = 88.8$, $P < 0.001$). 43% of recaptured nematodes had moved into the arms towards plant roots, 57% remained in the central pot. Mean ($\pm$ standard error) abundance is shown ($n = 11$). (b) Number of trichodorids moving towards infected plants in relation to viral load in the roots of those plants. TRV-infected plants with greater viral load attracted more trichodorids when tested against uninfected plants (linear regression, $P < 0.01$, $r^2 = 0.49$).

vector trichodorids and, thereby, potentially promote transmission of the virus from plant to plant. Infection with TRV significantly modifies both root morphology and the profile of volatile emissions from the roots, specifically enhancing 2-ethyl-1-hexanol production. Both trichodorid chemotaxis and 2-ethyl-1-hexanol production correlated strongly with plant viral load, while the addition of 2-ethyl-1-hexanol to uninfected plants made them significantly more attractive to trichodorids than untreated counterparts. Removal of TRV RNA2-encoded 2b and 2c genes significantly reduced the production of 2-ethyl-1-hexanol and trichodorid attraction. This is the first demonstration of attraction through semiochemicals in vector nematode–plant interactions and the existence of such novel belowground multitrophic signalling could have significant implications for both soil ecology and the management of agricultural pests.

Viral infection impacts on root morphology and the release of volatiles from infected roots

Our first hypothesis, that viral infection would impact root growth and the release of root volatiles and that this would reflect the viral load within the roots was supported. The changes in root morphology corresponded to levels of virus infection, with the maximum differences in root growth parameters occurring between wt-infected plants and uninfected plants at 7 and 14 dpi and were not apparent by 21 dpi, corresponding to the levels of infection detected at these time points. The recovery of *N. benthamiana* from TRV infection is a known phenomenon, although in other plants, such as in potato tubers, the virus can remain as a viable but very low-level infection for long periods (Sahi *et al.*, 2016). Research has shown that the steep reduction in levels of TRV in infected plants is the result of an interaction between the TRV RNA1-encoded 16K protein and the plant nuclear protein coilin, leading to the activation of specific plant defence pathways (Shaw *et al.*, 2019).

Wild-type TRV infection drives a temporary reduction in root biomass, with commensurately diminished root surface area, length, and volume. While trichodorids are named 'stubby root nematodes' (Decraemer, 1995) due to their root feeding with

resultant malformation of plant root tips, our results suggest that, in this study system at least, it is TRV infection that initiates the reduction in root biomass and associated structural parameters. The successful transmission of TRV requires that the virus is collected during an initial trichodorid feeding event and then deposited during a second feeding into a different part of the plant or, more productively, into roots of another plant. The feeding process is destructive, with the nematode depositing glandular secretions into the plant cell that liquefy the cell contents enabling them to be removed through the stylet and into the nematode oesophagus (Taylor & Brown, 1997). It is assumed that transmission of the virus occurs during interrupted feeding or sensory probing events that do not kill the recipient cell. These results challenge our perception of the drivers of a critical functional outcome within plant-virus-nematode vector systems; further research is needed to determine whether this phenomenon occurs in other plant virus–vector nematode systems.

2-ethyl-1-hexanol is produced in healthy *N. benthamiana* plants; however, during the period of maximum infection (7 dpi), wt TRV-infected plants produced significantly more 2-ethyl-1-hexanol than uninfected plants and emissions, like the impacts on root morphology, were tightly correlated with viral load. 2-ethyl-1-hexanol is a known anthropogenic chemical, and the limited production observed in uninfected and mutant plants cannot be ruled out as methodological contaminants. However, 2-ethyl-1-hexanol production in plants is known to result from an array of biotic attacks and stresses, such as beetle herbivory (Heil & Bueno, 2007), fungal parasitism (Castelyn *et al.*, 2015), and pathogenic bacteria (Yi *et al.*, 2009) but, until now, the overproduction of 2-ethyl-1-hexanol due to nematode-mediated virus infection has not been reported.

Attraction of trichodorid nematodes to infected plants in response to changes in root volatiles

We have demonstrated, for the first time, that TRV-infected *N. benthamiana* are more attractive to trichodorids than are uninfected plants and that 2-ethyl-1-hexanol release is a critical component of the attraction. Plants infected with wt virus released
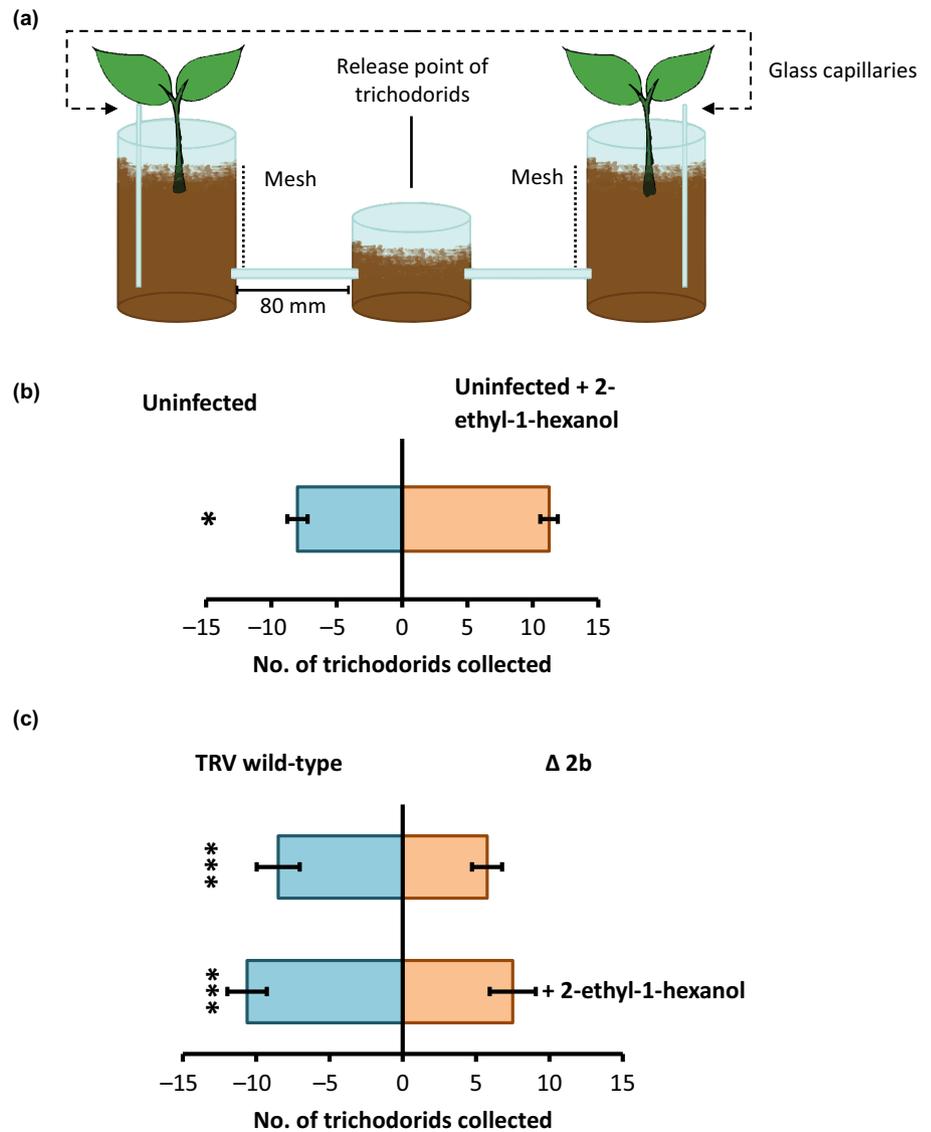
Fig. 7 Response of trichodorid nematodes presented with uninfected plants and those with added 2-ethyl-1-hexanol. (a) Revised olfactometer design with glass capillaries for addition of 2-ethyl-1-hexanol to plant roots. (b) Preference of trichodorids between uninfected plants with or without the addition of 2-ethyl-1-hexanol. Means and standard errors are shown ($n = 8$). There was significantly greater trichodorid movement towards uninfected plants with added 2-ethyl-1-hexanol (GLIM-p $\chi^2_{(2,21)} = 12.4$, $P < 0.05$). (c) Preference of trichodorids between plants infected with either wild-type TRV or TRVΔ2b, with and without 2-ethyl-1-hexanol. Means and standard errors are shown ($n = 8$). In both trials, there was a significant movement towards plants infected with wild-type TRV. *, $P < 0.05$; ***, $P < 0.001$.

more 2-ethyl-1-hexanol and were more attractive to trichodorids than were uninfected plants. This supports our second hypothesis that the observed difference in the attraction of trichodorids to plants infected with TRV compared with uninfected plants is due to the difference in volatile signals caused by TRV infection. Furthermore, we have shown that the addition of 2-ethyl-1-hexanol to uninfected plants is sufficient to attract more trichodorids to these plants compared with uninfected, untreated plants, again suggesting that 2-ethyl-1-hexanol plays a significant role in the attraction of trichodorids to TRV-infected plants. We recognise that we have not eliminated the possibility that larger compounds, including non-volatile organics, could have been modified in, or generated by, root tissues and this could be an explanation for the reduced impact of the addition of 2-ethyl-1-hexanol on nematode behaviour in the experiments with the 2b mutant. Non-volatile compounds are less likely to be influential however, since diffusion rates through water are substantially slower than through the vapour phase, and the gap between planted olfactometer section and nematodes was 8 cm.

Substantial nematode movement towards uninfected plants remained even without the addition of 2-ethyl-1-hexanol. We have shown that uninfected plants do not release appreciable amounts of 2-ethyl-1-hexanol from their roots, so this observed attraction cannot be fully explained by this compound, suggesting that while 2-ethyl-1-hexanol acts as an important cue for trichodorids, other signals may contribute to their attraction to plant roots. For example, some nematodes respond to basic environmental cues indicating the presence of roots, such as CO_2 gradients (Turlings *et al.*, 2012). Root volatiles are complex mixtures, which respond to abiotic and biotic stresses in targeted ways, with potential impact on nematode behaviours (Sikder & Vestergård, 2020). The 2-ethyl-1-hexanol emissions that we report were elevated in wt TRV infection on a $g\,g^{-1}$ root mass basis, but all other root volatiles that we observed were not significantly different between treatments. However, observed changes in root morphology after infection are likely to influence the strength and prevalence of these signals, whether they are gaseous (e.g. CO_2) or liquid (e.g. soil moisture content) in nature.

Mutations in TRV RNA 2 genes and their impact on volatile production and trichodorid nematode attraction

Tobacco rattle virus carrying mutations in the 2b and 2c genes produced similar, though generally slightly less severe (particularly in the case of Δ2c), changes in root morphology to that resulting from wt TRV infection. This was not our prediction, but, in line with our third hypothesis, infection by virus with these mutations did significantly reduce the production of 2-ethyl-1-hexanol by plants, such that the rate of volatile emissions no longer differed from uninfected plants and in the case of Δ2c, no longer correlated with viral load. This was reflected in trichodorid behaviour, with plants infected with TRV Δ2b significantly less attractive to trichodorids than plants infected with wt TRV, and this difference, while reduced, was maintained when 2-ethyl-1-hexanol was added to the pot containing the Δ2b mutant virus.

Whether volatile signals generated by infected plants are directly induced by infection as a modification of existing plant metabolism, as a plant stress response, or as a by-product of infection remains unclear. The TRV RNA 2b and 2c are relatively small proteins with no identifiable structural similarity to known metabolic proteins (MacFarlane, 2010), so it appears unlikely that they are directly responsible for changes in VOC production in TRV-infected plants. Nevertheless, several plant virus-encoded proteins are known to modify plant metabolic and regulatory processes. (Hyodo & Okuno, 2020). For example, in cucumber mosaic virus, the (unrelated to TRV) 2b gene encodes a small protein that inhibits host defences (Ziebell et al., 2011) and alters host *N. tabacum* VOC emissions (Tungadi et al., 2017). There is evidence that the 2b protein of TRV is multifunctional. It was found that TRV carrying the 2b gene and GFP as a reporter gene had an increased ability to infect and persist in roots, root meristems, and shoot meristems as compared with TRV carrying only GFP (Valentine et al., 2004). Accompanying this, the 2b-containing TRV initiated a longer lasting and more widespread virus-induced gene-silencing response, which has since been exploited for functional genomics studies in roots (Wang et al., 2022).

Our VOC analyses show that 2-ethyl-1-hexanol is an important cue for attracting trichodorid nematodes to the plant roots and that the TRV 2b protein has an unexplained role in affecting the production of these chemicals. Once the nematode has been stimulated to begin feeding on the root cells, virus transmission likely relies on physical interaction between the virus particle and specific regions of the nematode oesophagous, an idea supported by the use of TRV Coat Protein (CP)-specific immunogold electron microscopy to demonstrate that TRV particles are localised at the nematode oesophageal surface (Karanastasi et al., 2000). Molecular virology studies have clearly implicated the TRV 2b protein in this part of the transmission process, in a role separate to its action on VOC production; these studies, using combination of TRV strains with and without mutations in the 2b gene, suggest the 2b protein binds to the TRV coat protein to provide a link between the virus particle and the nematode oesophagus (Vellios et al., 2002; Holeva & MacFarlane, 2006).

The fact that the addition of 2-ethyl-1-hexanol did not make plants infected with the Δ2b mutant as attractive to nematodes as plants infected with wt TRV suggests this compound is not the sole driver of plant–nematode interactions but may be part of a more complex cocktail of chemical cues produced by TRV-infected plants. Plants infested by biotic agents, including arthropods (Peñaflor et al., 2011) and nematodes (Hallem et al., 2011) produce a variety of compounds from infected roots and nematode behaviour has been shown to be most strongly influenced by application of intact root exudate mixtures (Wang et al., 2018). While the full spectrum of volatiles from infected plants appears to induce the greatest response, our experiments have shown that 2-ethyl-1-hexanol is an important chemoattractant for nematodes and is a significant component of the total volatile signal to which trichodorids respond.

Conclusion

TRV–trichodorid interactions sit at the confluence of plant virus–vector relationships, nematode chemotaxis, and plant-mediated rhizosphere signalling. Work on plant virusvector interactions is dominated by studies on aboveground arthropod vectors, but unlike aboveground interactions, nematode vectors can only rely on chemical and physical gradients to orient themselves towards plants. This work demonstrates that a plant virus with a nematode vector uses chemical signals to attract virus vectors and has identified a critical component of that signal. These findings are valuable for our understanding of nematode chemotaxis, advancing our knowledge of virus transmission in arable production systems, and generating novel information on chemically mediated plant–soil biota interactions. We propose that this particular chemical interaction between virus, nematode vector, and crop plant could be the basis of a nature-based solution, to be incorporated within an integrated pest management framework, to mitigate the effects of nematode–virus transmission in potato. These results provide an example of critical soil interactions and provide insights into an important knowledge gap within soil ecology.

Competing interests

None declared.

Author contributions

SEH, KRR, SM and P-AG designed the experiments; P-AG, KRR, SM and RN developed the methodology; P-AG and KRR carried out the experiments and analysed the data; RN provided the hand-picked nematodes; SM provided TRV viruses; P-AG,

ORCID

Sue E. Hartley ⓘ https://orcid.org/0000-0002-5117-687X
Stuart A. MacFarlane ⓘ https://orcid.org/0000-0002-6046-4400
Roy Neilson ⓘ https://orcid.org/0000-0003-4544-2227
Kelly R. Redeker ⓘ https://orcid.org/0000-0002-1903-2286

Data availability

The authors confirm that the data supporting the findings of this study are available within the article and its Supporting Information.

References

Bardgett RD, van der Putten WH. 2014. Belowground biodiversity and ecosystem functioning. *Nature* **515**: 505–511.

Beuch U, Persson P, Edin E, Kvarnheden A. 2014. Necrotic diseases caused by viruses in Swedish potato tubers. *Plant Pathology* **63**: 667–674.

Bezemer TM, De Deyn GB, Bossinga TM, van Dam NM, Harvey JA, Van der Putten WH. 2005. Soil community composition drives aboveground plant–herbivore–parasitoid interactions. *Ecology Letters* **8**: 652–661.

Boutsika K, Phillips MS, MacFarlane SA, Brown DJF, Holeva RC, Blok VC. 2004. Molecular diagnostics of some trichodorid nematodes and associated *Tobacco rattle virus*. *Plant Pathology* **53**: 110–116.

Bouwmeester H, Schuurink RC, Bleeker PM, Schiestl F. 2019. The role of volatiles in plant communication. *The Plant Journal* **100**: 892–907.

Brown DJF, Boag B. 1988. An examination of methods used to extract virus-vector nematodes (Nematoda: Longidoridae and Trichodoridae) from soil samples. *Nematologia Mediterranea* **16**: 93–99.

Castelyn HD, Appelgryn JJ, Mafa MS, Pretorius ZA, Visser B. 2015. Volatiles emitted by leaf rust infected wheat induce a defence response in exposed uninfected wheat seedlings. *Australasian Plant Pathology* **44**: 245–254.

Chitwood DJ. 2003. Research on plant-parasitic nematode biology conducted by the United States Department of Agriculture-Agricultural Research Service. *Pest Management Science* **59**: 748–753.

Christie JR, Perry VG. 1951. A root disease of plants caused by a nematode of the genus *Trichodorus*. *Science* **113**: 491–493.

De Wang M, Deyn MB, Bezemer TM. 2019. Separating effects of soil microorganisms and nematodes on plant community dynamics. *Plant and Soil* **441**: 455–467.

Decraemer W. 1995. *The family Trichodoridae: stubby root and virus-vector nematodes.* Dordrecht, the Netherlands: Kluwer Academic Publishers, 1–360.

Eigenbrode SD, Bosque-Perez NA, Davis TS. 2018. Insect-borne plant pathogens and their vectors: ecology, evolution, and complex interactions. *Annual Review of Entomology* **63**: 169–191.

Fereres A, Peñaflor M, Favaro C, Azevedo K, Landi C, Maluta N, Bento J, Lopes J. 2016. Tomato infection by whitefly-transmitted circulative and non-circulative viruses induce contrasting changes in plant volatiles and vector behaviour. *Viruses* **8**: 225.

Hallem EA, Dillman AR, Hong AV, Zhang Y, Yano JM, DeMarco SF, Sternberg PW. 2011. A sensory code for host seeking in parasitic nematodes. *Current Biology* **21**: 377–383.

Harrison BD, Robinson DJ. 1978. The tobraviruses. *Advances in Virus Research* **23**: 25–77.

Heil M, Bueno JCS. 2007. Within-plant signaling by volatiles leads to induction and priming of an indirect plant defense in nature. *Proceedings of the National Academy of Sciences, USA* **104**: 5467–5472.

Hernández C, Visser PB, Brown DJF, Bol JF. 1997. Transmission of tobacco rattle virus isolate PpK20 by its nematode vector requires one of the two non-structural genes in the viral RNA2. *Journal of General Virology* **78**: 465–467.

Himmelbauer ML. 2004. Estimating length, average diameter and surface area of roots using two different image analyses systems. *Plant and Soil* **260**: 111–120.

Holeva RC, MacFarlane SA. 2006. Yeast two-hybrid study of Tobacco rattle virus coat protein and 2b protein interactions. *Archives of Virology* **151**: 2123–2132.

van den Hoogen J, Geisen S, Routh D, Ferris H, Traunspurger W, Wardle DA, de Goede RGM, Adams BJ, Ahmad W, Andriuzzi WS et al. 2019. Soil nematode abundance and functional group composition at a global scale. *Nature* **572**: 194–198.

Hyodo K, Okuno T. 2020. Hijacking of host cellular components as proviral factors by plant-infecting viruses. *Advances in Virus Research* **107**: 37–86.

Issitt TJ, Sweeney ST, Brackenbury WJ, Redeker KR. 2022. Sampling and analysis of low molecular weight volatile metabolites in cellular headspace and mouse breath. *Metabolites* **12**: 599.

Jones JT, Haegeman A, Danchin EGJ, Gaur HS, Helder J, Jones MGK, Kikuchi T, Manzanilla-López R, Palomares-Rius JE, Wesemael WML et al. 2010. Top 10 plant-parasitic nematodes in molecular plant pathology. *Molecular Plant Pathology* **14**: 946–961.

Jones RAC, Naidu RA. 2019. Global dimensions of plant virus diseases: current status and future perspectives. *Annual Review of Virology* **6**: 387–409.

Karanastasi I, Vassilakos N, Roberts IM, MacFarlane SS, Brown DJF. 2000. Immunogold localisation of tobacco rattle virus particles within the virus-vector nematode *Paratrichodorus anemones*. *Journal of Nematology* **32**: 5–12.

Kleiber C, Zeileis A. 2008. *Applied econometrics with R.* New York, NY, USA: Springer-Verlag. [WWW document] URL https://CRAN.R-project.org/package=AER/ [accessed 1 October 2021].

Laufer M, Mohammad H, Maiss E, Richert-Pöggeler K, Dall'Ara M, Ratti C, Gilmer D, Liebe S, Varrelmann M. 2018. Biological properties of Beet soil-borne mosaic virus and Beet necrotic yellow vein virus cDNA clones produced by isothermal *in vitro* recombination: insights for reassortant appearance. *Virology* **518**: 25–33.

Lazarova S, Coyne D, Rodríguez MG, Peteira B, Ciancio A. 2021. Functional diversity of soil nematodes in relation to the impact of agriculture – a review. *Diversity* **13**: 64.

Liu D, Shi L, Han C, Yu J, Li D, Zhang Y. 2012. Validation of reference genes for gene expression studies in virus-infected *Nicotiana benthamiana* using quantitative real-time PCR. *PLoS ONE* **7**: e46451.

Liu YL, Schiff M, Marathe R, Dinesh-Kumar SP. 2002. Tobacco *Rar1*, *EDS1* and *NPR1/NIM1* like genes are required for *N*-mediated resistance to tobacco mosaic virus. *The Plant Journal* **30**: 415–429.

Low JC, Wang N-Y, Williams J, Cicerone RJ. 2003. Measurements of ambient atmospheric C_2H_5Cl and other ethyl and methyl halides at coastal California sites and over the Pacific Ocean. *Journal of Geophysical Research-Atmospheres* **108**: 4608.

MacFarlane SA. 1999. The molecular biology of the tobraviruses. *Journal of General Virology* **80**: 2799–2807.

MacFarlane SA. 2008. *Tobravirus in encyclopedia of virology, 3rd edn.* Cambridge, MA, USA: Academic Press, 72–76.

MacFarlane SA. 2010. Tobraviruses – plant pathogens and tools for biotechnology. *Molecular Plant Pathology* **11**: 577–583.

MacFarlane SA, Neilson R. 2009. Testing of transmission of tobraviruses by nematodes. *Current Protocols in Microbiology* Chapter 16, **Unit 16B.5**: 1–16.

MacFarlane SA, Vassilakos N, Brown DJ. 1999. Similarities in the genome organization of tobacco rattle virus and pea early-browning virus isolates that are transmitted by the same vector nematode. *Journal of General Virology* **80**: 273–276.

MacFarlane SA, Wallis CV, Brown DJF. 1996. Multiple virus genes involved in the nematode transmission of PEBV. *Virology* **219**: 417–422.

Mauck KE, Chesnais Q. 2020. A synthesis of virus-vector associations reveals important deficiencies in studies on host and vector manipulation by plant viruses. *Virus Research* **285**: 197957.

Mauck KE, De Moraes CM, Mescher MC. 2010. Deceptive chemical signals induced by a plant virus attract insect vectors to inferior hosts. *Proceedings of the National Academy of Sciences, USA* **23**: 3600–3605.

McMenemy LS, Hartley SE, MacFarlane SA, Karley AJ, Shepherd T, Johnson SN. 2012. Raspberry viruses manipulate the behaviour of their insect vectors. *Entomologia Experimentalis et Applicata* 144: 56–68.

Mueller AM, Mooney AL, MacFarlane SA. 1997. Replication of *in vitro* tobravirus recombinants shows that the specificity of template recognition is determined by 5′ non-coding but not 3′ non-coding sequences. *Journal of General Virology* 78: 2085–2088.

Nibau C, Gibbs DJ, Coates JC. 2008. Branching out in new directions: the control of root architecture by lateral root formation. *New Phytologist* 179: 595–614.

Otulak K, Chouda M, Chrzanowska M, Garbaczewska G. 2012. Ultrastructural effects of infection caused by Tobacco rattle virus transmitted by *Trichodorus primitivus* in potato and tobacco tissues. *Canadian Journal of Plant Pathology* 34: 126–138.

Peñaflor MFGV, Erb M, Miranda LA, Werneburg AG, Bento JMS. 2011. Herbivore-induced plant volatiles can serve as host location cues for a generalist and a specialist egg parasitoid. *Journal of Chemical Ecology* 37: 1304–1313.

Pickett JA, Khan ZR. 2016. Plant volatile-mediated signalling and its application in agriculture: successes and challenges. *New Phytologist* 212: 856–870.

Ploeg AT, Brown DJF, Robinson DJ. 1992. The association between species of *Trichodorus* and *Paratrichodorus* vector nematodes and serotypes of tobacco rattle tobravirus. *Annals of Applied Biology* 121: 619–630.

R Core Team. 2020. *R: a language and environment for statistical computing.* Vienna, Austria: R Foundation for Statistical Computing. [WWW document] URL https://www.R-project.org/ [accessed 1 October 2021].

Raguso RA, Agrawal AA, Douglas AE, Jander G, Kessler A, Poveda K, Thaler JS. 2015. The raison d'être of chemical ecology. *Ecology* 96: 617–630.

Rasmann S, de Vos M, Casteel CL, Tian D, Halitschke R, Sun JY, Agrawal AA, Felton GW, Jander G. 2012. Herbivory in the previous generation primes plants for enhanced insect resistance. *Plant Physiology* 158: 854–863.

Ratcliff F, Martin-Hernandez AM, Baulcombe DC. 2001. Technical advance: tobacco rattle virus as a vector for analysis of gene function by silencing. *The Plant Journal* 25: 237–245.

Redeker KR, Cai LL, Dumbrell AJ, Bardill A, Chong JPJ, Helgason T. 2018. Non-invasive analysis of the soil microbiome: biomonitoring strategies using the volatilome, community analysis and environmental data. *Advances in Ecological Research* 59: 93–132.

Sahi G, Hedley PE, Morris J, Loake GJ, MacFarlane SA. 2016. Molecular and biochemical examination of Spraing disease in potato tuber in response to *Tobacco rattle virus* infection. *Molecular Plant–Microbe Interactions* 29: 822–828.

Schulz-Bohm K, Gerards S, Hundscheid M, Melenhorst J, de Boer W, Garbeva P. 2018. Calling from distance: attraction of soil bacteria by plant root volatiles. *The ISME Journal* 12: 1252–1262.

Senthil-Kumar M, Mysore KS. 2014. Tobacco rattle virus-based virus-induced gene silencing in *Nicotiana benthamiana*. *Nature Protocols* 9: 1549–1562.

Shapiro L, De Moraes CM, Stephenson AG, Mescher MC. 2012. Pathogen effects on vegetative and floral odours mediate vector attraction and host exposure in a complex pathosystem. *Ecology Letters* 15: 1430–1438.

Shaw J, Yu C, Makhotenko A, Makarova SS, Love AJ, Kalinina NO, MacFarlane S, Chen J, Taliansky ME. 2019. Interaction of a plant virus-encoded protein with the structural Cajal body protein coilin facilitates salicylic acid-mediated plant defence response. *New Phytologist* 224: 439–453.

Sikder MM, Vestergård M. 2020. Impacts of root metabolites on soil nematodes. *Frontiers in Plant Science* 10: 1792.

Sikder MM, Vestergård M, Kyndt T, Fomsgaard IS, Kudjordjie EN, Nicolaisen M. 2021. Benzoxazinoids selectively affect maize root-associated nematode taxa. *Journal of Experimental Botany* 72: 3835–3845.

Taylor CE, Brown DJF. 1997. *Nematode vectors of plant viruses.* Wallingford, Oxon, UK: CABI Publishing.

Tungadi T, Groen SC, Murphy AM, Pate AE, Iqbal J, Bruce TJA, Cunniffe NJ, Carr JP. 2017. Cucumber mosaic virus and its 2b protein alter emission of host volatile organic compounds but not aphid vector settling in tobacco. *Virology Journal* 14: 91.

Turlings TCJ, Hiltpold I, Rasmann S. 2012. The importance of root-produced volatiles as foraging cues for entomopathogenic nematodes. *Plant and Soil* 358: 51–60.

Valentine T, Shaw J, Blok VC, Phillips MS, Oparka KJ, Lacomme C. 2004. Efficient virus-induced gene silencing in roots using a modified tobacco rattle virus vector. *Plant Physiology* 136: 3999–4009.

Vassilakos N, Vellios EK, Brown EC, Brown DJF, MacFarlane SA. 2001. Tobravirus 2b protein acts in trans to facilitate transmission by nematodes. *Virology* 279: 478–487.

Vellios EK, Duncan G, Brown DJF, MacFarlane SA. 2002. Immunogold localisation of tobravirus 2b nematode transmission helper protein associated with virus particles. *Virology* 300: 118–124.

Venturi V, Keel C. 2016. Signaling in the rhizosphere. *Trends in Plant Science* 21: 187–198.

Wang C, Masler EP, Rogers ST. 2018. Responses of *Heterodera glycines* and *Meloidogyne incognita* infective juveniles to root tissues, root exudates, and root extracts from three plant species. *Plant Disease* 102: 1733–1740.

Wang Y, Durairaj J, Suárez Duran HG, van Velzen R, Flokova K, Liao CY, Chojnacka A, MacFarlane S, Schranz ME, Medema MH et al. 2022. The tomato cytochrome P450 CYP712G1 catalyzes the double oxidation of orobanchol *en route* to the rhizosphere signaling strigolactone, solanacol. *New Phytologist* 235: 1884–1889.

War AR, Paulraj MG, Ahmad T, Buhroo AA, Hussain B, Ignacimuthu S, Sharma HC. 2012. Mechanisms of plant defense against insect herbivores. *Plant Signaling & Behavior* 7: 1306–1320.

Wiesel L, Daniell TJ, King D, Neilson R. 2015. Determination of the optimal soil sample size to accurately characterise nematode communities in soil. *Soil Biology and Biochemistry* 80: 89–91.

Wood SV, Maczey N, Currie AF, Lowry AJ, Rabiey M, Ellison CA, Jackson RW, Gange AC. 2020. Rapid impact of *Impatiens glandulifera* control on above- and belowground invertebrate communities. *Weed Research* 61: 35–44.

Yi H-S, Heil M, Adame-Álvarez R-M, Ballhorn D, Ryu M. 2009. Airborne induction and priming of plant resistance to a bacterial pathogen. *Plant Physiology* 151: 2152–2161.

Ziebell H, Murphy AM, Groen SC, Tungadi T, Westwood JH, Lewsey MG, Moulin M, Kleczkowski A, Smith AG, Stevens M et al. 2011. Cucumber mosaic virus and its 2b RNA silencing suppressor modify plant-aphid interactions in tobacco. *Scientific Reports* 1: 187.

Supporting Information

Additional Supporting Information may be found online in the Supporting Information section at the end of the article.

Fig. S1 Experimental design for semi-static headspace sampling with stainless steel canisters.

Fig. S2 Representative chromatograms from *Nicotiana benthamiana* root headspace samples with four different tobacco rattle virus infection regimes (uninfected, TRV wild-type, Δ2b, and Δ2c).

Table S1 Comparison between root growth and morphology parameters across a 28-d infection timeline for *Nicotiana benthamiana* plants infected with wild-type and mutant tobacco rattle virus.

Please note: Wiley is not responsible for the content or functionality of any Supporting Information supplied by the authors. Any queries (other than missing material) should be directed to the *New Phytologist* Central Office.